Third-order Optical Nonlinearities of Higher Fullerene and Carbon Nanotube

Rui-Hua Xie and Qin Rao[a]

Max-Planck-Institute für Strömungsforschung, Bunsenstr. 10, D-37073 Göttingen, Germany
[a] Nanchang Telecommunication Bureau, Nanchang 330003, People's Republic of China

Reprint requests to Dr. R.-H. X.; E-mail: rxie@gwdg.de

Z. Naturforsch. **54 a,** 645–658 (1999); received July 23, 1999

Recent theoretical and experimental studies on the third-order optical nonlinearities of higher fullerenes including C_{70}, C_{76}, C_{84}, C_{86}, C_{90}, C_{94} and C_{96} are briefly reviewed. The extended Su-Schrieffer-Heeger model is introduced and applied to study the third-order optical nonlinearity of chiral carbon nanotubes (CCN), where the average contribution Γ of one carbon atom to the third-order optical nonlinearity of each CCN is calculated and compared with that of a well characterized polyenic polymer. It is found that (i) the smaller the diameter of a CCN, the larger the average contribution Γ; (ii) the metallic CCN favors larger third-order optical nonlinearity than the semiconducting one; (iii) CCN can compete with the conducting polymer achieving a large third-order optical susceptibility. Also the doping effect on the second-order hyperpolarizability of a tubular fullerene is investigated. It is found that the doping effect increases greatly the magnitude of the second-order hyperpolarizability of tubular fullerene.

Key words: Optical Susceptibility; Hyperpolarizability; Sum-over-state Approach; Resonance Enhancement; C_{60}; Higher Fullerene; Tubular Fullerene; Carbon Nanotube; Chiral Effect; Doping Effect.

I. Introduction

It is known that molecules with large third-order optical nonlinearities, characterized by large second-order hyperpolarizabilities γ, are required for photonic applications including all-optical switching, data processing, and eye and sensor protection [1 - 11]. However, the γ magnitudes of most third-order optical materials are usually smaller than those required for photonic devices. Hence, recent research effort in physics, chemistry and engineering has been devoted to finding potential third-order materials with large nonlinear optical (NLO) response.

It has been shown, both theoretically and experimentally [1 - 9], that conjugated π-electron organic systems and quantum dots are potentially important in photonics owing to their large third-order optical nonlinearities. Recently, the advent of the technology for the production of bulk quantities of fullerenes C_n [12 - 14] and carbon nanotubes [12, 15 - 17] has provided us another class of completely conjugated materials, which have quantum dot nature and possess a large number of delocalized π-electrons but are uniquely composed of carbon atoms. A further desirable characteristic of these carbon materials in comparison with organic or polymer NLO material is that there is no C-H or O-H bond, which would otherwise induce absorption and limit their use in nonlinear optics. Naturally, these feature make fullerenes and carbon nanotubes appealing NLO materials for photonic applications and stimulates the theoretical and experimental researchers in physics, chemistry and engineering to study the third-order optical nonlinearities of fullerenes and carbon nanotubes.

The extensive studies were triggered by the first experimental measurement on the third-order optical nonlinearity of C_{60} by Blau et al. [18] in 1991, although it was later found out that an error by more than three orders of magnitude for the final hyperpolarizability was incorporated in their measurements [19, 20]. This error seems to be quite indicative of the later development with numerous measurements using different experimental techniques obtaining data for the third-order optical susceptibilities $\chi^{(3)}$ of C_{60} [21 - 41]. In Table I we collect some of the reported third-order optical susceptibilities $\chi^{(3)}_{xxxx}$ of

Table I. Third-order optical susceptibilities $\chi^{(3)}_{xxxx}$ (in units of 10^{-13}esu) of C_{60} measured by different experimental techniques, where λ (μm) is the wavelength.

λ	$\chi^{(3)}_{xxxx}$	Technique	Year	Ref.
0.532	1	DFWM	1998	[59]
0.85	150	THG	1992	[22]
1.06	70	DFWM	1992	[24]
	600000	DFWM	1991	[18]
	33000	DFWM	1992	[23]
	140	THG	1992	[27]
	2000	THG	1991	[21]
	820	THG	1992	[22]
	720	THG	1992	[29]
1.32	300	THG	1992	[27]
	610	THG	1992	[22]
1.50	300	THG	1992	[29]
1.91	160	EFISHG	1992	[26]
	90	THG	1992	[27]
	320	THG	1992	[22]
2.00	370	THG	1992	[29]
2.37	40	THG	1992	[27]

C_{60} at a few selected wavelengths λ measured by degenerate four-wave mixing (DFWM), third-harmonic generation (THG), or electric-field-induced second-harmonic generation (EFISHG). It is important to recognize that because the third-order optical responses are very sensitive to many experimental factors such as the measurement techniques adopted, the incident laser power, and even the sample preparation method, it is rather difficult for us to make a direct comparison of experimental results on nonlinear optical properties of C_{60} obtained from different groups by different experimental techniques. In general, there is reasonable agreement between the experimental values of $\chi^{(3)}_{xxxx}$ of C_{60} measured by THG and EFISHG, although some variation in the magnitudes of $\chi^{(3)}_{xxxx}$ is apparent (other reviews on the nonlinear optical properties of C_{60} are also available in the recent literatures, for example, by Nalwa [7], Rustagi et al. [10], and Belousov et al. [11]). In spite of the discrepancy of several orders in the third-order optical susceptibilities existing in the experimental data, it has recently been shown that C_{60} possesses a small value of the second-order hyperpolarizability [42, 43]. An upper bound of $3.7\times10^{-35}esu$ of the second-order hyperpolarizability for C_{60} was measured by nondegenerate four-wave mixing by Geng and Wright [42], and a 9.0×10^{-35}esu upper limit was determined by the femtosecond optical Kerr effect (OKE) by Gong and his coworkers [43].

However, higher fullerenes, compared with C_{60}, have attracted less attention on their third-order optical nonlinearities. Theoretical calculations [33, 34, 36, 44 - 57] and a few experimental results [28, 29 - 31, 35, 37, 40, 58, 59] have shown that higher fullerenes possess a larger third-order optical nonlinearity than C_{60}. In the following section, we briefly review recent theoretical and experimental studies on the third-order optical nonlinearities of higher fullerenes. In Sect. III, we introduce the extended Su-Schrieffer-Heeger (SSH) model and apply it to study the third-order optical nonlinearity of the chiral carbon nanotube (CCN). In Sect. IV, by including the effect of dopant ions into the extended SSH model, we turn to study the substitute doping effect on the second-order hyperpolarizability of armchair tubular fullerenes. Finally, Sect. V presents our conclusion.

II. Third-order Optical Nonlinearity of Higher Fullerenes

A) Theoretical Calculations

Based on the geometries optimized by AM1 semiempirical technique [60], Shuai and Bredas [49] exploited the valence-effective-Hamiltonian (VEH) method to study the electronic structures of C_{60} and C_{70}. The valence-electronic density of states calculated is found to be in excellent agreement with the high-resolution energy-distribution curves obtained from synchrotron-photoemission experiments in terms of both positions and relative intensities of the peaks [49]. The maximum difference in peak position between theory and experiment is 0.4 eV, which shows that the VEH method provides a very reasonable description of both C_{60} and C_{70}. Further they applied the VEH-Sum-Over-State (SOS) approach to study the nonlinear optical response of C_{60} and C_{70}. Their numerical results showed that the off-resonance third-order optical susceptibility $\chi^{(3)}$ is on the order of 10^{-12} esu [49]. Their calculations are fully consistent with the EFISHG and THG measurements by Wang and Cheng [26] and the DFWM measurements by Kafafi et al. [20, 24], but about three to four orders of magnitude lower than the data reported by Blau et al. [18] and Yang et al. [30].

Recently, available theoretical studies predicted that the second-order hyperpolarizability of a higher fullerene scales with the mass of the all-carbon molecule [44, 47, 50 - 56]. Knize [44] applied the

free electron gas model to study the second-order hyperpolarizability of fullerene molecules. The magnitude of the calculated polarizabilities of C_{60} and C_{70} molecules were found to be in reasonable agreement with some of the experiments, and the second-order hyperpolarizability of the larger fullerene molecules is predicted to increase as the cube of the number of carbon atoms [44]. With the SOS-CNDO/S CI approach, a power dependence of the second-order hyperpolarizabilities of fullerenes versus the number of carbon atoms was observed by Fanti et al. [50], where the observed exponent is four. Then, using a sum-over-molecular-orbitals (SOMO) approach at the Hartree-Fock level with a $6-31G^*$ basis set, Fanti et al. [51] further calculated the static second-order hyperpolarizabilities of the eight carbon cages now available in macroscopic quantities: C_{60}, C_{70}, one isomer of C_{76}, three isomers (1,2,3) of C_{78}, and two isomers (22 and 23) of C_{84}. Concentrating on either the molecular mass (the number N of carbon atoms) or the number of partial double bonds ($\frac{3}{2}N-60$), they found two different scaling laws [51]:

$$\gamma^{(\text{mass})} = \left(\frac{N}{60}\right)^{3.5}\gamma^{60}, \tag{1}$$

$$\gamma^{(\text{bond})} = \left(\frac{\frac{3}{2}N-60}{30}\right)^{1.5}\gamma^{60}, \tag{2}$$

where γ^{60} is the static γ value of C_{60}. Later, based on the extended Su-Schrieffer-Heeger model, Xie and his coworkers predicted that the static γ values of armchair ($C_{60+i\times 10}$) and zigzag ($C_{60+i\times 18}$) tubular fullerenes of small size obey the exponent laws [52]

$$\gamma = \left(1+\frac{i\times 10}{60}\right)^{3.15}\gamma^{60}, \tag{3}$$

$$\gamma = \left(1+\frac{i\times 18}{60}\right)^{2.98}\gamma^{60}, \tag{4}$$

repsectively, and larger third-order optical nonlinearities of armchair and zigzag tubular fullerenes can be observed in the infrared region [45, 46]. Also Harigaya [53 - 56] theoretically investigated the nonlinear optical properties of C_{60}, extracted higher fullerenes C_{70}, C_{76}, C_{78}, and C_{84} by using the exciton formalism and the SOS method. It is found that the off-resonant third-order susceptibilities of higher fullerenes are a few times larger than those of C_{60} [53 - 56], where the magnitude of the optical nonlinearity increases as the optical gap decreases for higher fullerenes, and the optical nonlinearity is nearly proportional to the fourth power of the carbon number when the on-site Coulomb repulsion is $2t$ or $4t$ (t being the nearest-neighbour hopping integral). The theoretical calculations of both Xie [45, 46, 52] and Harigaya [53 - 56] indicate the important roles of Coulomb interactions in higher fullerenes and agree very well with quantum chemical calculations for higher fullerenes. Very recently, Luo [47] re-examine the reported data for the second-order hyperpolarizabilities of fullerenes calculated by Fanti et al. [51] and Jonsson et al. [36]. It is found that, if C_{60} is excluded, a perfect power law dependence for the second-order hyperpolarizability versus the number N of carbon atoms is observed [47]:

$$\gamma = \frac{11N^{2.4}}{100000} \tag{5}$$

for the data of Fanti et al. [51] and

$$\gamma = \frac{4N^{0.75}}{125} \tag{6}$$

for the data of Jonsson et al. [36]. Luo [47] also indicated that C_{60} has the most exceptional electron localization among fullerenes.

It is well-known that molecular symmetry has a great effect on the nonlinear optical properties of molecules. In order to identify this issue, of course, C_{78} would be very interesting and a better candidate for examing this effect than others since the C_{78} molecule has five topologically distinct structures: two with C_{2v} symmetry, two with D_{3h} symmetry, and one with D_3 symmetry, each having 29 six-membered rings and 12 five-membered rings. For convenience, the five isomers of C_{78} are denoted by $D_{3h}(1)$, $D_{3h}(2)$, D_3, $C_{2v}(2)$, $C_{2v}(1)$. Very recently, using the SOS method, Wan et al. [61] calculated the third-order optical nonlinearities for the five C_{78} isomers. Although the Coulomb interactions among π-electrons have not been taken into account, their numerical results really indicate that both the symmetry and the arrangement of atoms have great influences on the third-order optical nonlinearities of C_{78} isomers. It is found that the static γ values (in units of 10^{-32} esu) of $D_{3h}(1)$, $D_{3h}(2)$, D_3, $C_{2v}(1)$, and $C_{2v}(2)$ are 0.0480, 0.2096, 0.0681, 0.2034 and 0.0507, respectively [61]. As we know, the $D_{3h}(1)$ structure is

similar to the D_3 structure except that the former has one more symmetry plane than the latter, which makes its energy levels move to each other and the degeneracy of its energy levels be higher than that of D_3 isomer. But the THG spectra of the $D_{3h}(1)$ and D_3 isomers are greatly different due to their different symmetry. In the THG spectrum of the D_3 isomer, there is a big peak located at $3\omega = 6.08$ eV, and the γ magnitude is 342.49×10^{-32} esu [61]. However, in the THG spectrum of the $D_{3h}(1)$ isomer, the highest peak is at $3\omega = 6.592$ eV and the corresponding γ is 17.50×10^{-32} esu, which is 20 times smaller than that of D_3 [61]. Furthermore, they have also shown that the atom arrangement of the C_{78} isomers has a great effect on their NLO properties. We know that the $D_{3h}(1)$ and $D_{3h}(2)$ isomers have the same symmetry, but their arrangements of atoms are different. It is found that their THG spectra are different, too. In the THG spectrum of the $D_{3h}(1)$ isomer, the γ magnitude of the highest peak is only 17.50×10^{-32} esu [61]. In the THG spectrum of the $D_{3h}(2)$ isomer, its γ magnitudes at the frequency region, $2.944 \text{ eV} \leq 3\omega \leq 3.584$ eV, are greater than 80×10^{-32} esu and its largest γ reaches even 509.01×10^{-32} esu which is 30 times larger than that of the $D_{3h}(1)$ isomer [61]. Due to the shape effect, the γ magnitudes of $C_{2v}(2)$ and $C_{2v}(1)$ are also greatly different. In the THG spectrum of the $C_{2v}(1)$ isomer, there are three peaks with γ magnitudes greater than 50×10^{-32} esu, but the largest γ magnitude in the THG spectrum of the $C_{2v}(2)$ isomer is only 15.995×10^{-32} esu [61].

From a geometric point of view, Moore et al. [48, 57] analyzed the static third-order polarizabilities γ of C_{60}, C_{70}, five isomers of C_{78} and two isomers of C_{84} in terms of three properties: (i) symmetry; (ii) aromaticity; (iii) size. The polarizability values were based on the finite field approximation (FFA), using a semiempirical Hamiltonian, and applied to the molecular structures obtained from density functional theory calculations. Symmetry was characterized by the molecular group order. The selection of six-member rings as aromatic was determined from an analysis of bond lengths. The maximum interatomic distance and surface area were the parameters considered with respect to size. Based on triple linear regression analysis, it was found that the static linear polarizability α and second-order hyperpolarizability γ in these molecules respond differently to geometrical properties [48, 57]: α depends almost exclusively on the surface area, while γ is affected by a combination of the number of aromatic rings, length and group order, in decreasing importance. In the case of α, valence electron contributions provide the same information as all-electron estimates [48, 57]. For the second-order hyperpolarizability γ, the best correlation coefficients are obtained when all-electron estimates are used and when the dependent parameter is $\ln(\gamma)$ instead of γ [48, 57].

Table II. Static γ value of higher fullerenes calculated by different theoretical techniques.

Molecule	γ (10^{-37} esu)	Technique	Year	Ref.
C_{70}	452	FFA	1992	[34]
	8623	SOS	1992	[49]
	13000	SOS	1994	[33]
	8570	SOS	1995	[50]
	545	FFA	1996	[48]
	6400	SOS	1997	[45]
	2945	SOS	1997	[51]
	10500	SOS	1997	[61]
	754	RPA	1998	[36]
C_{76}	3681	SOMO	1997	[51]
$C_{78}(D_3)$	3619	SOMO	1997	[51]
	6810	SOS	1997	[61]
$C_{78}(C_{2v}(1))$	3699	SOMO	1997	[51]
	20340	SOS	1997	[61]
$C_{78}(C_{2v}(2))$	4407	SOMO	1997	[51]
	5070	SOS	1997	[61]
$C_{78}(D_{3h}(1))$	4800	SOS	1997	[61]
$C_{78}(D_{3h}(2))$	20960	SOS	1997	[61]
C_{84}	18120	SOS	1995	[50]
	636	FFA	1996	[48]
$C_{84}(D_2)$	4269	SOMO	1997	[51]
$C_{84}(D_{2d})$	4606	SOMO	1997	[51]
C_{84}	824	RPA	1998	[36]
$C_{60+9\times10}$	85000	SOS	1998	[45]
$C_{60+5\times18}$	68600	SOS	1998	[46]

Very recently, Jonsson et al. [36] have studied the third-order optical nonlinearities of C_{60}, C_{70}, and C_{84} on the random phase approximation (RPA) level with a 6-31++G basis set. The calculated static γ values for C_{60}, C_{70}, and C_{84} are 55.0, 75.4, 82.4×10^{-36} esu, respectively.

In Table II we collect the static second-order hyperpolarizabilities of higher fullerenes calculated by different theoretical techniques. A direct comparison between the calculated results shows significant differences. It seems that all of the SOS approaches give a second-order hyperpolarizability which is about an order of magnitude larger than that predicted by the *ab initio* calculations. This discrepancy may arise from the truncation of the expansion in excited states in the explicit summation of contributions to the second-

order hyperpolarizability in SOS calculations [36]. In contrast, the second-order hyperpolarizabilities obtained in the FFA methods[48, 34] are of the same order of magnitude. The described problems are absent in the analytical RPA approach [36].

B) Experimental Measurements

Neher et al. [29] studied the second-order hyperpolarizabilities γ of the buckminsterfullerenes C_{70} at three different wavelengths measured by THG in a toluene solution, and the third-order optical susceptibilities $\chi^{(3)}_{xxxx}$ of C_{70} at 1.06, 1.50 and 2.00 μm were determined to be 1.4×10^{-9} esu, 5.4×10^{-10} esu, and 9.1×10^{-11}esu, respectively. Their experimental results were compared with those of C_{60}. Based on this, they observed strong effects with γ exceeding 5×10^{-32} esu in the three-photon resonant regime.

Wang and Cheng [26] reported the determination of the second- and third-order optical nonlinearities of fullerenes and fullerene/N,N-diethylaniline (DEA) charge-transfer complexes by solution-phase DC EFISHG measurements with 1.91-μm radiation. The third-order polarizabilities, $\gamma_{1111}(-2\omega, \omega, \omega, 0)$, of C_{60} and C_{70} were determined to be $(7.5 \pm 2) \times 10^{-34}$ esu and $(1.3 \pm 0.3) \times 10^{-33}$ esu, respectively. They also found that the second-order polarizabilities of fullerenes are zero due to their centrosymmetric structures. However, the formation of charge-transfer complexes with N, N-diethylaniline breaks the center of symmetry and induces second-order optical nonlinearity. The dipole projection of the second-order polarizability, β_μ, of the C_{60}/DEA charge-transfer complex was determined to be $(6.7 \pm 2) \times 10^{-29}$ esu, assuming $\gamma_{1111}(-2\omega, \omega, \omega, 0)$ to be approximately the same in toluene and DEA [26]. With due consideration to molecular size, the optical nonlinearities of fullerenes are comparable to those of linearly conjugated organics. Their experimental results are encouraging enough to warrant further study of the nonlinear optical properties of fullerenes and properly substituted fullerene derivatives.

Kafafi and coworkers [31, 37] studied the third-order optical nonlinearities of C_{60} and C_{70}. Time-resolved DFWM experiments were conducted on films of pure C_{60} and C_{70} by using a picosecond tunable dye laser. The fullerenes exhibit a two-photon resonantly enhanced third-order optical response which is primarily laser-pulse-limited [37], their dynamics show wavelength and fluence dependence[31], and in detail the third-order optical susceptibilities $\chi^{(3)}_{xxxx}$ (in units of 10^{-11} esu) of C_{70} at 1.064, 0.675, and 0.597 μm are measured to be 1.2 [37], 64 ± 20 [31], and 210 ± 10[31], respectively.

Gong and his coworkers [30] studied the nonlinear third-order optical susceptibility of C_{70} in a toluene solution which was measured for the first time by the method of DFWM using 10 ns laser pulses at 1.06 μm. The third-order susceptibility $\chi^{(3)}_{1111}$ was measured to be 5.6×10^{-12} esu for a C_{70} toluene solution at a concentration of 0.476 g/l. The corresponding magnitude of the second-order hyperpolarizability γ_{1111} of the C_{70} molecule is 1.2×10^{-30} esu.

Thin film of pure C_{70} has also been studied by time-resolved DFWM using femtosecond optical pulses with a wavelength of 0.633 μm [35]. Large optical nonlinearities of C_{70} were measured with $\chi^{(3)}_{xxxx} = 3 \times 10^{-10}$ esu at 0.633 μm.

Sun et al. [40] studied the third-order optical nonlinearity of C_{84} by using the time-resolved optical Kerr effect (OKE). They got a large instantaneous nonlinear optical response of C_{84} using 150-fs laser pulses with a wavelength of 647 nm. Comparing the nonlinear optical response with that of the CS_2 reference, they acquired a large second-order hyperpolarizability for C_{84},C_{70} and C_{60} with γ_{1111} of 5.2×10^{-31}, 4.7×10^{-31}, and 1.6×10^{-31} esu, respectively [40]. In contrast to the γ_{1111} increment of C_{70} to C_{60}, the small accretion of the optical Kerr response of C_{84} in comparison to C_{70} seems to be a puzzle. It is claimed that the sample purity was not satisfactory [58]. In their experiment, C_{84} was obtained from fullerite soot. The separation and purification were carried out by means of liquid phase chromatography combined with a recrystallization technique. Their NMR spectra showed that the main impurities include C_{78}, C_{82}, C_{86} and C_{90}, although the purity of C_{84} was greater than 85%.

Recently, Yang and his coworkers[58] have made DFWM measurements on the third-order optical nonlinearities of the higher purity C_{90} (> 97% in their mass spectrum) and C_{60}. They reported that C_{90} shows a large third-order nonlinear optical response at 0.532 μm in comparison to that of C_{60}. The concentration of the fullerenes and the incident laser power were found to be vitally important in the DFWM measurements and were therefore optimized. They measured the UV-VIS absorption spectra of C_{60} and C_{90} in CS_2. Their spectrum of C_{60} is identical with that of Diederich et al. [62], confirming the high purity of their sample. The spectrum of C_{90} exhibits the

strongest peak around 450 nm in the spectral range 400 - 800 nm. It is apparent from a comparison of the two spectra that the long wavelength absorption edge is significantly red-shifted from C_{60} to C_{90}. This may be attributed to the narrowing of the HOMO-LUMO gap due to the increased size of the π-conjugated system and the reduction in the fullerene symmetry. Since their excitation wavelength (0.532 μm) is near the absorption peaks of C_{60} and C_{90}, the linear absorption should not be ignored in their DFWM measurements. From the set of $\chi^{(3)}_{1111}$ values, the second-order hyperpolarizability of C_{90} was determined to be $(1.8 \pm 0.6) \times 10^{-30}$ esu through a statistical analysis in which three times the standard deviation ($\pm 3\sigma$) was taken for the uncertainty [58]. For comparison, the second-order hyperpolarizability of C_{60} was measured to be $(2.2 \pm 0.6) \times 10^{-31}$ esu using the same procedure. Since there are more highly delocalized π-conjugated electrons over the spherical-like surface in C_{90} compared to C_{60}, the larger γ value of C_{90} is expected. Surely, the eightfold increase in the third-order optical polarizability from C_{60} to C_{90} is consistent with the trend in the theoretical predictions [50 - 56]. However, the predicted increase in the second-order hyperpolarizability γ from C_{60} to C_{90} is somewhat lower than the measured eightfold increase. This suggests that other factors contributing to the increased second-order hyperpolarizability may be important as well.

Furthermore, Yang and his coworkers [59] have systematically studied the nonlinear optical response of other higher fullerenes including C_{76}, C_{78}, C_{84}, C_{86}, C_{94} and C_{96} by performing the DFWM measurement on those fullerene series dissolved in CS_2. The DFWM measurements were carried out using 70 ps laser pulses at a wavelength of 0.532 μm under optimized experimental conditions. The second hyperpolarizabilities γ_{1111} (in units of 10^{-30} esu) of C_{60}, C_{70}, C_{76}, C_{78}, C_{84}, C_{86}, C_{94} and C_{96} were determined to be 0.22 ± 0.06, 1.3 ± 0.4, 0.8 ± 0.3, 1.5 ± 0.3, 1.2 ± 0.3, 1.3 ± 0.5, 1.9 ± 0.6, and 2.1 ± 0.6, respectively [59], and the ratios for the second-order hyperpolarizabilities for C_{70}/C_{60}, C_{84}/C_{60}, and C_{84}/C_{70} were found to be 3.63, 5.45 and 0.92, respectively, where overall they increase smoothly with the carbon cage size except for C_{70} and C_{78}. Their experiments confirmed the high nonlinear efficiency of C_{70} and they found that C_{78} possesses a larger γ than the other fullerene cages. The number of π-conjugated electrons, geometrical structure, and resonance enhancement were discussed as possible factors responsible for the observed third-order optical nonlinearities of the fullerenes [59].

Table III. Third-order optical susceptibilities $\chi^{(3)}_{xxxx}$ (in units of 10^{-13} esu) of higher fullerenes measured by different experimental techniques, where λ (μm) is the wavelength.

C_n	λ	$\chi^{(3)}_{xxxx}$	Technique	Year	Ref.
C_{70}	0.532	4.3	DFWM	1998	[59]
	0.597	21000	DFWM	1992	[31]
	0.633	3000	DFWM	1992	[35]
	0.647	87000	OKE	1995	[40]
	0.675	6400	DFWM	1992	[31]
	1.064	120	DFWM	1993	[37]
		56	DFWM	1992	[30]
		14000	THG	1992	[29]
	1.50	5400	THG	1992	[29]
	1.91	440	EFISHG	1992	[26]
	2.00	910	THG	1992	[29]
C_{76}	0.532	2.8	DFWM	1998	[59]
C_{78}	0.532	5.5	DFWM	1998	[59]
C_{84}	0.532	3.9	DFWM	1998	[59]
	0.647	80000	OKE	1995	[40]
C_{86}	0.532	4.9	DFWM	1998	[59]
C_{90}	0.532	7.2	DFWM	1997	[58]
C_{94}	0.532	6.0	DFWM	1998	[59]
C_{96}	0.532	6.7	DFWM	1998	[59]

Table III collects some experimental data obtained by different measurements on the third-order optical nonlinearities of higher fullerenes discussed above.

III. Third-Order Optical Nonlinearity of Chiral Carbon Nanotubes

Bisides the armchair and zigzag tubules[12], a large number of chiral carbon nanotubes (CCNs) [12] can be formed with a screw axis along the axis of the tubule and with a variety of "hemispherical"-like caps. These carbon nanotubes can be specified mathematically in terms of the tubule diameter d_t and chiral angle θ, as shown in Fig. 1 where the chiral vector

$$\boldsymbol{C}_h = p\boldsymbol{a}_1 + q\boldsymbol{a}_2 \tag{7}$$

is shown as well as the basic translation vector $\boldsymbol{T}$ for CCN. The vector $\boldsymbol{C}_h$ connects two crystallographically equivalent sites O and A on a two-dimensional graphene structure. The construction in Fig. 1 shows the chiral angle θ of the tubule with respect to the zigzag direction ($\theta = 0$) and two units, $\boldsymbol{a}_1$ and $\boldsymbol{a}_2$, of the hexagonal honeycomb lattice. An ensemble of possible chiral vectors can be specified by $\boldsymbol{C}_h$ in terms

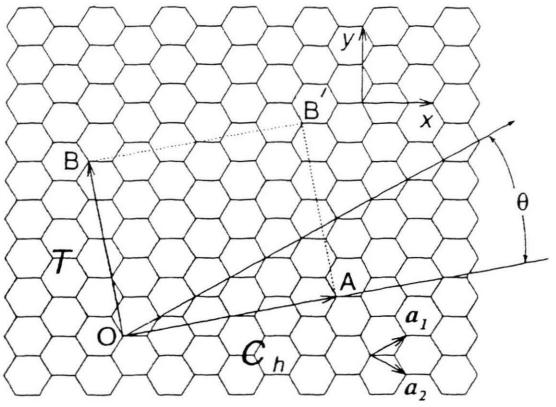

Fig. 1. The chiral vector OA or $\boldsymbol{C}_h = p\boldsymbol{a}_1 + q\boldsymbol{a}_2$ is defined on the honeycomb lattice of carbon atoms by the unit vectors $\boldsymbol{a}_1$ and $\boldsymbol{a}_2$ and he chiral angle θ with respect to the zigzag axis (θ = 0). Also shown is the lattice vector $\boldsymbol{T} = OB$ of the 1D tubule unit cell.

of pairs of integers (p, q) [12, 63 - 65]. Each pair of integers (p, q) defines a different way of rolling the graphene sheet to form a carbon nanotube. In detail, the cylinder connecting the two hemispherical caps of the armchair, zigzag, or chiral tubule is formed by superimposing the two ends OA of the vector $\boldsymbol{C}_\mathrm{h}$. The cylinder joint shown in Fig. 1 is made by joining the line AB' to the parallel line OB, where lines OB and AB' are perpendicular to the vector $\boldsymbol{C}_\mathrm{h}$ at each end. The CCN thus generated has no distortion of bond angles other than distortions caused by the cylindrical curvature of the CCN. Differences in the chiral angle θ and the tubule diameter d_t give rise to differences in the properties of the various carbon nanotubes. In the (p, q) notation for specifying the chiral vector $\boldsymbol{C}_\mathrm{h}$, the vectors $(p, 0)$ denote zigzag tubules, and the vectors (q, q) denote armchair tubules, and all other vectors (p, q) correspond to CCNs [12, 63 - 65]. In terms of the integers (p, q), the tubule diameter d_t is given by [12]

$$d_\mathrm{t} = C_\mathrm{h}/\pi = \frac{\sqrt{3(p^2 + pq + q^2)}}{\pi} a_{\mathrm{C-C}}, \tag{8}$$

where $a_{\mathrm{C-C}}$ is the nearest-neighbor C-C distance (= 1.421 Å in graphite [12]), $\mathrm{C_h}$ is the length of the chiral vector $\boldsymbol{C}_\mathrm{h}$, and the chiral angle θ is given by [12]

$$\theta = \tan^{-1}\left(\frac{\sqrt{3}q}{q + 2p}\right). \tag{9}$$

Let m be the largest common divisor in p and q. Then, the atom number n per unit cell is equal to

$$n = \frac{4(p^2 + pq + q^2)}{m} \tag{10}$$

if $(p - q)$ is not a multiple of $3m$, or

$$n = \frac{4(p^2 + pq + q^2)}{3m} \tag{11}$$

if $(p - q)$ is a multiple of $3m$.

Based on their experimental observations, Iijima and co-workers [66] claimed that most of single-walled carbon nanotubes show chirality. Using a similar technique to Iijima's, Dravid et al. [67] also found that most of their carbon nanotubes have a chiral structure. Therefore, it is very interesting to examine the chiral effect on the third-order optical nonlinearities of CCNs in the view of their practical application.

The Su-Schrieffer-Heeger (SSH) model [68] has been successfully applied to describe conducting polymers and C_{60} [69 - 71]. Since the Coulomb interaction effect plays an important role in the physical understanding of the electronic and optical properties of higher fullerenes and carbon nanotubes, we have recently extended the SSH model, where the Coulomb interaction is included, to describe higher fullerenes and C_{60}-based nanotubes [45, 46, 52]. The total Hamiltonian can be written as [45, 46, 52]

$$\begin{aligned}\mathcal{H} = & \sum_{\langle ij\rangle}\sum_{s}\left(-t_0 - \alpha_0 y_{ij}\right)\left(c^\dagger_{i,s}c_{j,s} + \mathrm{h.c.}\right) \\ & + \frac{k_0}{2}\sum_{<ij>} y_{ij}^2 + u_0\sum_i c^\dagger_{i,\uparrow}c_{i,\uparrow}c^\dagger_{i,\downarrow}c_{i,\downarrow} \\ & + v_0\sum_{<ij>}\sum_{s,s'} c^\dagger_{i,s}c_{i,s}c^\dagger_{j,s'}c_{j,s'},\end{aligned} \tag{12}$$

where the sum $\langle ij\rangle$ is taken over the nearest neighbors for the C-C bond, t_0 represents the hopping integral for the C-C bond, α_0 the electron-phonon coupling constant related to the C-C bond, k_0 the spring constant corresponding to the C-C bond, y_{ij} the change of the bond length between the ith and jth atom; the operator $\mathrm{C}_{i,s}$ ($\mathrm{C}^\dagger_{i,s}$) annihilates (creates) a π electron at the ith atom with spin s ($s = \uparrow, \downarrow$), u_0 is the usual on-site Coulomb repulsion strength, and v_0 is the Coulomb interaction between the nearest and next-nearest atoms.

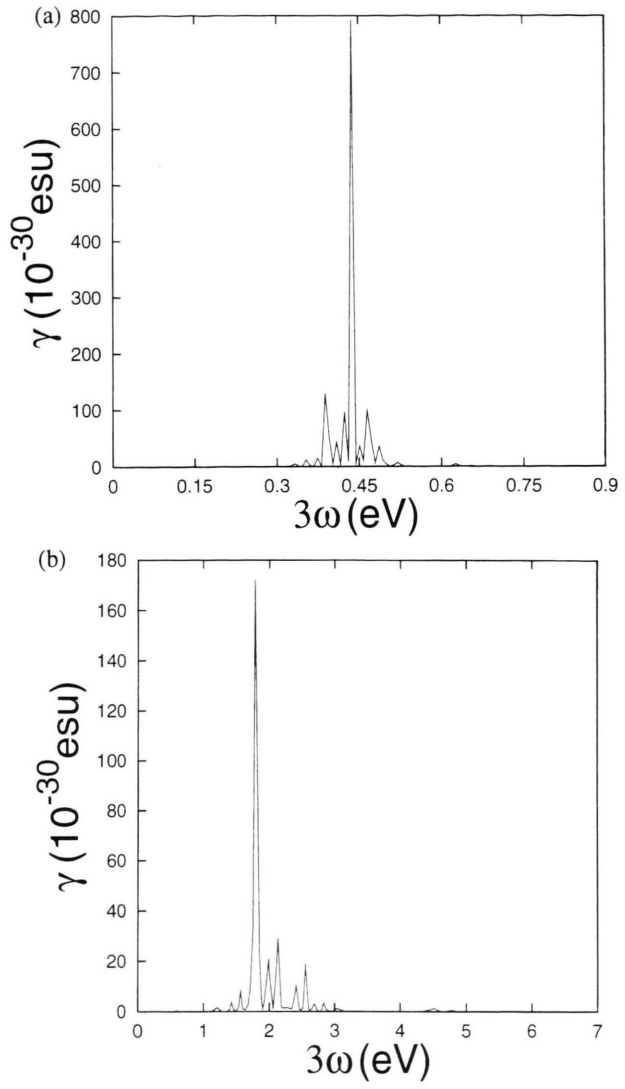

Fig. 2. The second-order hyperpolarizability γ spectra of a single substituted armchair tubular fullerene. (a) $C_{(60+9\times10)-1}N$ (E_g = 0.136 eV) and (b) $C_{(60+9\times10)-1}B$ (E_g = 0.647 eV), where E_g is the energy gap of the corresponding tubule.

Within the SOS approach discussed by Orr and Ward [72], the second-order hyperpolarizability γ for the THG process can be written as [see Fig. 2 of [73], taking into account six diagrams in total]

$$\gamma(-3\omega;\omega,\omega,\omega) = \gamma_2 + \gamma_3 + \gamma_1 + \gamma_4 + \gamma_7 + \gamma_8, \quad (13)$$

where γ_i is given in [49]. Since the ratios between different components of γ are not known, a spatial average of γ is given by [48]

$$\gamma = \frac{\gamma_{xxxx} + \gamma_{yyyy} + \gamma_{zzzz} + 2\gamma_{xxyy} + 2\gamma_{yyzz} + 2\gamma_{zzxx}}{5}. \quad (14)$$

Here we turn to study CCNs with finite atom numbers N. In these cases the tubule edge effects cannot be neglected. A finite CCN with one or several unit cells is open with a row of dangling bonds at each end. So an atom at an edge site may have fewer than three neighbors. However, for the real carbon nanotubes, the tubule length is long enough to neglect the edge effect. Taking this into account, we have applied periodic boundary condition for the tubule axis, and each carbon atom at the end of the finite CCN can still find its three neighbors by imagining that the two ends of the tubule are connected. In Fig. 1, a unit cell is defined along the tubule axis, and $\boldsymbol{C}_h$ and $\boldsymbol{T} = OB$ construct the basis vectors of the unit cell, where B is the first lattice point of the 2D graphitic sheet through which a line through O and perpendicular to $\boldsymbol{C}_h$ passes. Based on the electronic structures obtained in the above model, we calculate the static γ values of 17 CCNs, which have different diameter d_t and chiral angle θ. Then, we calculate the average contribution Γ of one carbon atom to the third-order optical nonlinearity of a CCN,

$$\Gamma = \frac{\gamma}{N}, \quad (15)$$

where N is the total atom number in the studied CCN. We note that for carbon nanotubes with smaller diameters than that of C_{60} there are no caps containing only pentagons and hexagons which can be fitted continuously to such a small carbon nanotube (p, q). For this reason it is expected that the observation of very narrow (< 7 Å) carbon nanotubes is very unlikely [12, 15]. For example, the (4,2) chiral vector does not have a proper cap and therefore is not expected to correspond to a physical carbon nanotube. Therefore, in view of practical application, we pay our attention to physical tubules including the (6,5) tubule which is the smallest diameter CCN. In detail, our numerical results are listed in Table IV. Therein we have also given the corresponding diameter d_t, the chiral angle θ, the atom number n per unit cell, and the total atom number N in the calculated tubule, from which we may examine the effect of size, chiral angle, and diameter on the third-order optical nonlinearities of the CCN. In Table IV, s and m in $(p, q)^s$ and $(p, q)^m$

Table IV. The static γ (in units of 10^{-33} esu) value and average contribution Γ (in units of 10^{-35} esu) of the 17 chiral carbon nanotube, where s and m in $(p, q)^s$ and $(p, q)^m$ denote semiconducting and metallic nanotubes, respectively. n, N, d_t (Å), and θ are the atom number per unit cell, the total atom number calculated, the diameter, and the chiral angle of a chiral carbon nanotube, respectively.

(p, q)	n	N	d_t	θ	γ	Γ
C_{60}	–	60	7.10	–	0.5612	0.9353
$(6,5)^s$	364	364	7.47	0.4711	6.3556	1.7461
$(9,1)^s$	364	364	7.47	0.0909	5.1997	1.4285
$(7,4)^m$	124	372	7.56	0.3674	22.9996	6.1827
$(8,3)^s$	388	388	7.72	0.2669	5.4013	1.3921
$(9,2)^s$	412	412	7.95	0.1715	5.7198	1.3883
$(7,5)^s$	436	436	8.18	0.4276	6.0172	1.3801
$(10,1)^m$	148	444	8.25	0.0822	25.0398	5.6396
$(8,4)^s$	112	448	8.29	0.3334	6.1766	1.3787
$(9,3)^m$	156	468	8.47	0.2425	22.1879	4.7419
$(10,2)^s$	248	496	8.72	0.1561	6.7049	1.3518
$(7,6)^s$	508	508	8.83	0.4792	6.8504	1.3485
$(8,5)^m$	172	516	8.90	0.3911	18.1596	3.5193
$(9,4)^s$	532	532	9.03	0.3050	6.9155	1.2999
$(10,3)^s$	556	556	9.24	0.2221	6.8811	1.2376
$(8,6)^s$	296	592	9.53	0.4413	6.8157	1.1513
$(9,5)^s$	604	604	9.68	0.3601	6.7642	1.1199
$(10,4)^m$	104	624	9.79	0.2810	14.8830	2.3851

denote the semiconducting and metallic CCNs, respectively.

It has been shown that the optical nonlinearities of fullerenes decrease with increasing space dimensions. For example, the 3D C_{60} molecule possesses smaller γ values than a 1D conducting polymer with the same number of atoms. The substitute doping effect reduces the effective space dimension of C_{70}, and thus their optical nonlinearities are greatly enhanced [85]. Here we see that the 1D CCN will roughly become a 2D graphite sheet with increase of its diameter. So it is expected that the smaller the diameter of a CCN, the larger its γ value. Table IV tells us that the Γ value for semiconducting CCN $(p, q)^s$ increases with decreasing diameters, i. e., the average contribution of one carbon atom to the third-order optical nonlinearity of a semiconducting CCN is gradually enhanced with the decrease of its diameter. A similar conclusion is got for metallic CCNs.

From Table IV, we know that $(6, 5)^s$ and $(9, 1)^s$ have the same diameter (d_t = 7.47 Å) and the same atom number per unit cell (n = 364) as well as semiconducting properties. The only difference between these two CCNs is the chiral angle θ (θ = 0.4711 for $(6, 5)^s$ and θ = 0.0909 for $(9, 1)^s$). In this case, if the total atom number N is the same, both CCNs will have the same height but the length of the base helix of $(6, 5)^s$ is shorter than that of $(9, 1)^s$. Thus, the atoms in $(6, 5)^s$ are situated along a more straight line than those in $(9, 1)^s$, and thus $(6, 5)^s$ has lower space dimensions than $(9, 1)^s$. Therefore we expect that $(6, 5)^s$ possesses a larger γ value than $(9, 1)^s$. From Table IV, we find that the Γ value of $(6, 5)^s$ is bigger than that of $(9, 1)^s$, i. e., the γ value of $(6, 5)^s$ is larger than that of $(9, 1)^s$ if their total atom number N is the same.

Table V. Seven different molecular weights (MW) with the experimentally derived γ (in units of 10^{-33} esu) values of a well characterized polyenic polymer, where Γ (in units of 10^{-35} esu) is the average contribution of a carbon atom to the third-order optical nonlinearity of the polymer. The number N of carbon atoms is obtained from the molecular weight by dividing by 12 and rounding up the result to the closest integer multiple of 10.

MW	N	γ	Γ
2800	230	3.5	1.5
4100	340	5.4	1.6
5400	450	7.8	1.7
7500	620	15.5	2.5
10000	830	26.7	3.2
17600	1460	62.9	4.3
27900	2320	85.4	3.7

The periodic boundary conditions for the 1D CCNs permit only a few wave vectors to exist in the circumferential direction [12]. If one of these passes through the zone corner in the Brillouin zone, then metallic conduction results; otherwise the CCN is semiconducting and has a band gap. Recently it has been shown that when the total atom number N of a carbon nanotube is increased greatly, a large energy gap for a semiconducting CCN is still available, but the energy gap for a metallic CCN approaches zero [12]. In this case it is expected that, if the total number N of carbon nanotubes is the same, a metallic CCN possesses a larger γ value than a semiconducting one. It is seen from Table IV that the Γ value of a metallic CCN is larger than that of a semiconducting CCN. Finally, comparing the Γ value of C_{60} with that of carbon nanotubes, we see that the carbon nanotube has a larger Γ value than C_{60}. This means that carbon nanotubes possess a larger NLO response than C_{60}.

Well characterized conjugated π-electron organic systems are important materials for nonlinear optics because their typically large third-order optical nonlinearities make them likely candidates for components of technological devices. As an example, in

Table V, we list the experimentally derived γ values and the average contributions Γ of a well characterized polyenic polymer for seven different molecular weights [74]. Comparing their Γ values with our calculated ones for 17 CCNs, one may find that CCNs also predict much higher NLO responses and can compete with polyenes for nonlinear optical applications. Since CCNs are uniquely composed of carbon atoms and therefore do not have any residual infrared absorption which the polymeric materials possess due to overtones of C-H stretching vibrations, they will be ideal candidates among all third-order materials for photonic applications. During the recent years, large quantities of single-walled [75] and multi-walled [12, 15 - 17] carbon nanotubes have been produced by experimental researchers. Despite this progress, a number of physical properties of single- or multi-walled carbon nanotubes have not been examined carefully so far. In particular, this applies to the nonlinear optical properties of carbon nanotubes, which determine the nonlinear dependence of the polarizability of carbon nanotubes on the intensities of incident electromagnetic waves. In the view of photonic applications, experimental studies on the NLO properties of carbon nanotubes are expected to be performed.

Very recently, Ye and his coworkers [76] have studied the third-order optical nonlinearity of carbon nanotubes by using the technique of backward DFWM. The light source was an Nd:YAG laser with a 30-ps-wide single pulse output or an Nd:YAG laser with an 8-ns-wide single pulse output. The wavelengths used in the experiments for each laser were 1064 and 532 nm. The magnitudes for the tensor component $\chi^{(3)}_{1111}$ of their solutions and solvent were measured via a comparison with that of reference sample CS_2. First, the typical absorption spectrum of carbon nanotubes, after they removed the contribution of the solvent, was measured with one of their solutions. They found that there exists some absorption at both 1064 nm and 532 nm [76]. Then, with the 30 ps laser, $\chi^{(3)}_{1111}$ was obtained for their solutions and solvent at both 1064 nm and 532 nm. They observed that $\chi^{(3)}_{1111}$ of all their solutions was larger than that of the solvent, and especially that a linear concentration dependence of $\chi^{(3)}_{1111}$ exists for their solutions at both 1064 nm and 532 nm. By subtracting $\chi^{(3)}_{1111}$ of the solvent from that of their solutions, $\chi^{(3)}_{1111}$ of carbon nanotubes in different solutions can be obtained. Typical results for one of their solutions at 1064 nm and 532 nm are 6.460×10^{-14} esu and 6.303×10^{-14} esu, respectively [76]. The results of similar experiments by using an 8-ns-wide laser at 1064 nm and 532 nm are 1.179×10^{-11} esu and 0.309×10^{-11} esu, respectively [76]. Since it is very difficult to know the exact number of carbon nanotubes solved in their solution because of the difficulty in obtaining carbon nanotubes with the same size, they could not calculate the third-order optical nonlinearity of a single nanotube. But instead, from the mass of carbon solved in the solution, they evaluated the average contribution of one carbon atom to the third-order optical nonlinearity of carbon nanotubes. As shown before, one result of $\chi^{(3)}_{1111}$ of carbon nanotubes at 1064 nm is about 6.460×10^{-14} esu, and considering the local field correction, they found that the average contribution Γ per carbon atom to the third-order optical nonlinearity of the carbon nanotube is about 0.6×10^{-35} esu [76]. For C_{60}, whose γ_{1111} is 3.0×10^{-34} esu at 1064 nm [24], the average contribution Γ per atom to the third-order optical nonlinearity of C_{60} is 0.5×10^{-35} esu. Clearly, the average contribution of one carbon atom in carbon nanotubes is longer than that in C_{60}. Enhancement of the third-order optical nonlinearity occurs in carbon nanotubes. This conclusion agrees with our above theoretical prediction.

IV. Third-order Optical Nonlinearity of Doped Tubular Fullerenes

Recently, doped fullerenes [12] and carbon nanotubes [77] have stimulated a great interest of physicists and chemists to investigate their structural, electronic, optical and other properties. Besides the alkali metal doping, there is another type of doping, named *substitute doping* (SD), i. e., substituting one or more carbon atoms of fullerenes and carbon nanotubes by other atoms. For example, boron and nitrogen atoms have been successfully used to replace carbon atoms of fullerenes [12] and carbon nanotubes [77]. Available studies [18 - 87] have shown that the lattice and electronic structures of fullerenes change with substituted doping; the band gaps between the highest occupied molecular orbitals (HOMO) and lowest unoccupied molecular orbitals (LUMO) and the electronic polarization of the substituted fullerenes vary greatly with different SD; the distribution of π-electrons on the surface of a fullerene is changed due to the SD effect; the original delocalized π-electrons

in the pure fullerene become more localized around the substituted atoms. Obviously, these factors have also a large effect on the NLO properties of fullerenes and carbon tubules. Therefore it would be interesting and useful to investigate theoretically the SD effect on the NLO properties of fullerenes [85] and carbon nanotubes [86, 87] from the view point of practical application. In this section we pay our attention to the doping effect on the third-order optical nonlinearity of armchair tubular fullerenes.

The above extended SSH model has been used to describe higher (and tubular) fullerenes and CCNs. But it should be modified to include the effect of the dopant ions in order to describe the substituted fullerenes and carbon nanotubes. The total Hamiltonian for the single substituted tubules can be written as [85, 86, 87]

$$\mathcal{H} = H^{(0)}_{\mathrm{C-C}} + H^{(1)}_{\mathrm{X-C}}, \tag{16}$$

$$\begin{aligned} H^{(0)}_{\mathrm{C-C}} = & \sum_{\langle ij\rangle}\sum_{s}\left(-t_0 - \alpha_0 y_{ij}\right)\left(c^{\dagger}_{i,s}c_{j,s} + \mathrm{h.c.}\right) \\ & + \frac{k_0}{2}\sum_{\langle ij\rangle} y^2_{ij} + u_0\sum_i c^{\dagger}_{i,\uparrow}c_{i,\uparrow}c^{\dagger}_{i,\downarrow}c_{i,\downarrow} \\ & + v_0\sum_{\langle ij\rangle}\sum_{s,s'} c^{\dagger}_{i,s}c_{i,s}c^{\dagger}_{j,s'}c_{j,s'}, \end{aligned} \tag{17}$$

$$\begin{aligned} H^{(1)}_{\mathrm{X-C}} = & \sum_{\langle ij\rangle}\sum_{s}\left(-t_1 - \alpha_1 y_{ij}\right)\left(c^{\dagger}_{i,s}c_{j,s} + \mathrm{h.c.}\right) \\ & + \frac{k_1}{2}\sum_{\langle ij\rangle} y^2_{ij} + u_1\sum_i c^{\dagger}_{i,\uparrow}c_{i,\uparrow}c^{\dagger}_{i,\downarrow}c_{i,\downarrow} \\ & + v_1\sum_{\langle ij\rangle}\sum_{s,s'} c^{\dagger}_{i,s}c_{i,s}c^{\dagger}_{j,s'}c_{j,s'}, \end{aligned} \tag{18}$$

where X denotes the substituted atom, and the sum $\langle ij\rangle$ is taken over the nearest neighbors for both the C-C and X-C bonds. t_0 (t_1), α_0 (α_1), and k_0 (k_1) represent the hopping integrals, the electron-phonon coupling constants and the spring constants corresponding to the C-C (X-C) bonds, respectively. u_0 (u_1) is the usual on-site Coulomb repulsion strength, and v_0 (v_1) is the Coulomb interaction between the nearest and next-nearest atoms. Since there is only one substituted impurity atom (i. e., X) in tubules, $H^{(1)}_{\mathrm{X-C}}$ plays a perturbational role, and as an approximation the original empirical parameters ($t_0, \alpha_0, k_0, u_0, v_0$) in $H^{(0)}_{\mathrm{C-C}}$ are assumed not to change due to the substitute doping (taken to be the same in this numerical calculation as those in the pure cases), $u_1 \approx u_0$, and $v_1 \approx v_0$.

Table VI. The ratio $q = \gamma^{\mathrm{im}}/\gamma^{\mathrm{p}}$ of several doped armchair tubular fullerenes, where γ^{im} is the calculated static γ value of the doped tubule $C_{(60+i\times 10)-1}X$ (X= B or N), γ^{p} is the static γ value of the corresponding pure case and given by the empirical formula $\gamma^{\mathrm{p}} = (1 + i \times 10/60)^{3.15}\gamma^{60}$, and $\gamma^{60} = 5.6 \times 10^{-34}$ esu is the static γ value of C_{60}.

X	$i = 0$	$i = 1$	$i = 2$	$i = 9$	$i = 18$
N	30.5	30.7	32.4	36.8	41.2
B	3.9	4.3	4.9	7.6	8.5

The choice of the three parameters (t_1, α_1, k_1) for the X-C bonds is important [85 - 87]. The best way to do it is to determine them by comparison between theoretical calculations and experimental measurements. But to the best of our knowledge, there has not been an experimental measurement on the nonlinear optical properties of doped carbon tubules. Recently, by using a molecular orbital method with Harris functional and spin-restricted approximations [88], where the total electron density of the system can be approximated by a superposition of electron densities of the isolated atoms with a first-order energy correction of the density error and quadratic errors in the electron Coulomb repulsion and exchange-correlation energies are partially canceled, Kurita et al. [80] have optimized the structures of $C_{59}N$ and $C_{59}B$ and at the same time investigated their electronic properties. They found that the optimized structures and binding energies for $C_{59}N$ and $C_{59}B$ were almost the same as those for C_{60}, and the energy levels near the Fermi level were remarkably changed by doping. In our recent work [85 - 87], by using the above theoretical model, we also investigated the structural and electronic properties of the same substituted doped fullerenes by carefully adjusting the values of the three parameters (t_1, α_1, and k_1). It is found that our numerical calculations can accurately reproduce the results obtained by Kurita et al. if $t_1 = 1.17$ eV, $\alpha_1 = 6.04$ eV/Å, and $k_1 = 51.1$ eV/Å^2 for $C_{59}B$, and $t_1 = 1.05$ eV, $\alpha_1 = 6.13$ eV/Å, and $k_1 = 49.6$ eV/Å^2 for $C_{59}N$.

Based upon the electronic structure obtained in the above theoretical model, we calculated the static second-order hyperpolarizabilities (γ^{im}) of the single substituted armchair ($C_{(60+i\times 10)-1}X$) tubular fullerenes, where X = B or N. The results are shown

in Table VI. Here the x axis is directed to the impurity ion X. In order to see the substitute doping effect on the NLO response of tubular fullerenes, we list the ratio q between γ^{im} and γ^{p} in the table:

$$q = \frac{\gamma^{\text{im}}}{\gamma^{\text{p}}}, \tag{19}$$

where γ^{p} denotes the static γ value of the corresponding pure case, which is given by the empirical formula $\gamma^{\text{p}} = (1 + i \times 10/60)^{3.15}\gamma^{60}$ for armchair tubular fullerenes [52] and $\gamma^{60} = 5.6 \times 10^{-34}$ esu is the static γ value of C_{60}. It is seen that the static γ value of $C_{(60+i\times 10)-1}B$ is several times larger than that of the corresponding pure one; and the static γ value of $C_{(60+i\times 10)-1}N$ is more than 30 times larger than that of the corresponding pure one. This means that substitute doping, especially for the case of X = N, greatly increases the nonlinear optical polarizability of carbon tubules. Here it should be mentioned that owing to the distortion of the π-electron distribution in the substituted tubules, especially around the substituted dopant B or N, the difference between the z and x (or y) components of γ for those substituted tubules is much more pronounced than that for pure cases.

The dynamical nonlinear optical response of a doped armchair tubule $C_{(60+9\times 10)-1}X$ has also been investigated by calculating the THG spectrum, and the results are shown in Figs. 2(a) and (b) for X = N, B, respectively. The first peaks appearing in Figs. 2(a) and (b) are located at $3\omega = 0.129$, and 0.653 eV, respectively, and their corresponding γ magnitudes are 47.9 and 25.3×10^{-32} esu, which are three and 1.6 times larger than that (= 15.6×10^{-32} esu [45, 46]) of pure armchair tubules. As in the pure case, we find that the first peak in the γ spectrum of the substituted armchair tubule is also caused by a three-photon resonance between two energy levels (a and b) near Fermi levels with one in the conduction band and the other in the valence band.

Moreover, Fig. 2(a) and (b) show that the highest peaks in the γ spectra are located at $3\omega = 0.437, 1.783$ eV, respectively, and their corresponding γ_{max} magnitudes are about 792.45×10^{-30} esu and 172.18×10^{-30} esu, which are about 60 and 13 times larger than that (= 13.44×10^{-30} esu [45, 46]) of the highest peak of the pure armchair tubule. These peaks are caused by one-, two-, and three-photon resonance enhancement. The other peaks with larger γ magnitudes are produced by two- or three-photon resonance. For example, in Fig. 2(a), the three-photon peaks with larger γ are located at $3\omega = 0.387, 0.423, 0.465$ eV, and the two-photon peaks with large γ are located at $3\omega = 0.409, 0.451, 0.487$ eV. Also we notice from Fig. 2(a) and (b) that the major response peaks with large γ concentrate on a narrow region, where the optical frequency is near the energy gap. The reason is the same as that for the pure case, i. e., a lot of one-, two-, and three-photon resonance enhancement processes can be observed in the doped tubule, but only those transition processes that occur between the energy levels near Fermi levels are able to contribute large γ magnitudes.

Based on our previous calculation, we know that the substituted dopant ions (X = B or N) attract or repel electrons [85, 86, 87] and thus may cause a distortion of the π-electron distribution on the tubule's surface, which mainly happens around the dopant ions (this effect can be called an inductive effect). On the other hand, the dopant ions cause greater localization of the original delocalized π-electrons around them, and therefore may reduce the effective space dimensions of fullerene tubules (this effect can be called reduction effect). Our numerical results have shown that both effects make the NLO properties of the substituted tubule different from the corresponding pure one and enlarge greatly its γ magnitudes. In addition, the localization effect of the N impurities is stronger than that of the B ones [85 - 87]. So the inductive and reduction effects of the effective space dimension in the nitrogen-doped tubule are stronger than those in boron-doped tubule, which explains why a nitrogen-doped tubule has larger γ values than a boron-doped one. Surely, it would be very interesting to see what would happen if heavier substitute doping is done. Based on the calculated results, this process will raise the γ magnitude further.

V. Conclusion

In this paper, we have reviewed recent theoretical and experimental studies on the third-order optical nonlinearities, characterized by the second-order hyperpolarizability γ, of higher fullerenes including C_{70}, C_{76}, C_{84}, C_{86}, C_{90}, C_{94} and C_{96}. The extended SSH model was introduced and applied to study the third-order optical nonlinearity of CCNs, where the average contribution Γ of one carbon atom to the third-order optical nonlinearity of each CCN is calculated and compared with that of a well characterized

polyenic polymer. It is found that the smaller the diameter of a CCN, the larger the average contribution Γ; the metallic CCN favors larger γ values than the semiconducting one; CCN can compete with the conducting polymer achieving a large γ value which is required for photonic applications. Then, by including the effect of dopant ions into the extended SSH model, we have studied the substitute doping effect on the static and dynamical second-order hyperpolarizabilities of armchair tubular fullerenes. It is found that the substitute doping effect increases greatly the γ magnitude of armchair tubular fullerene. Very recently, the generation of boron- or nitrogen-doped carbon nanotubes has been reported [77]. In the light of the experimental progress, the above theoretical studies are significant for photonic applications of those doped nanotubes.

Acknowledgements

We would like to thank Dr. K. Suenaga and Prof. Dr. Q. H. Gong for their reprints. R. H. X. and Q. R. acknowledge financial supports from Alexander von Humboldt Foundation and Nanchang Telecom Bureau, respectively.

[1] J. Messier, F. Kajzar, P. N. Prasad, and D. Ulrich, Nonlinear Optical Effects in Organic Polymers, Kluwer Academic, Dordrecht 1991.
[2] J. Messier, F. Kajzar, and P. N. Prasad, Organic Molecules for Nonlinear Optics and Photonics, Kluwer Academic, Dordrecht 1991.
[3] P. N. Prasad, and D. J. Williams, Introduction to Nonlinear Optical Effects in Molecules and Polymers, Wiley, New York 1991.
[4] J. I. Sakai, Phase Conjugate Optics, McGraw-Hill, Singapore 1992.
[5] H. S. Nalwa, Adv. Mater. **5**, 341 (1993).
[6] J. Zyss, Molecular Nonlinear Optics, Academic Press, New York 1994.
[7] H. S. Nalwa, Nonlinear Optical Properties of π-conjugated Materials, in: Handbook of Organic Conductive Molecules and Polymers, H. S. Nalwa ed., Wiley, New York 1997, Vol.IV, pp. 263-361.
[8] H. S. Nalwa, Organic Materials for Third-order Nonlinear Optics, in: Nonlinear Optics of Organic Molecules and Polymers, H. S. Nalwa and S. Miyata eds., CRC Press, Boca Raton, Florida 1997, Chapt. 11, pp. 611-797.
[9] U. Woggon, Optical Properties of Semiconductor Quantum Dots, Springer-Verlag, Berlin 1997.
[10] K. C. Rustagi, S. V. Nair, and L. M. Ramaniah, Progress in Crystal Growth & Characterization of Materials, **34**, 81 (1997).
[11] V. P. Belousov, I. M. Belousova, V. P. Budtov, V. V. Danilov, O. B. Danilov, A. G. Kalintsev, and A. A. Mak, Journal of Optical Technology, **64**, 1081 (1997).
[12] M. S. Dresselhaus, G. Dresselhaus, and P. C. Eklund, Science of Fullerenes and Carbon Nanotubes, Academic Press, San Diego 1996.
[13] H. W. Kroto, J. E. Fischer, and D. E. Cox, The Fullerenes, Pergamon Press, Oxford 1993.
[14] A. Hirsch, The Chemistry of the Fullerenes, Thieme, New York 1994.
[15] T. W. Ebbesen, Carbon Nanotubes, CRC Press, Boca Raton, Florida 1997.
[16] M. Endo, S. Iijima, and M. S. Dresselhaus, Carbon Nanotubes, Pergamon Press, Oxford 1996.
[17] P. M. Ajayan, and T. W. Ebbesen, Rep. Prog. Phys. **60**, 1025 (1997).
[18] W. J. Blau, H. J. Byme, D. J. Cardin, T. J. Dennis, J. P. Hare, H. W. Kroto, R. Taylor, and D. R. M. Walton, Phys. Rev. Lett. **67**, 1423 (1991).
[19] R. J. Knize, and J. P. Partanen, Phys. Rev. Lett. **68**, 2704 (1992).
[20] Z. H. Kafafi, F. J. Bartoli, J. R. Lindle, and R. G. S. Pong, Phys. Rev. Lett. **68**, 2705 (1992).
[21] H. Hoshi, N. Nakamura, Y. Maruyama, T. Nakagawa, S. Suzuki, H. Shiromaru, and Y. Achiba, Japan. J. Appl. Phys. **30**, L1397 (1991).
[22] F. Kajzar, C. Taliani, R. Zamboni, S. Rossini, and R. Danieli, Syhth. Met. **54**, 21 (1993).
[23] Q. Gong, Y. Sun, Z. Xia, Y. H. Zou, Z. Gu, X. Zhou, and D. Qiang, J. Appl. Phys. **71**, 3025 (1992).
[24] Z. H. Kafafi, J. R. Lindle, R. G. S. Pong, F. J. Bartoli, L. J. Lingg, and J. Milliken, Chem. Phys. Lett. **188**, 492 (1992).
[25] G. B. Talapatra, N. Manickam, M. Samoc, M. E. Orczyk, S. P. Karna, and P. N. Prasad, J. Phys. Chem. **96**, 5206 (1992).
[26] Y. Wang, and L. T. Cheng, J. Phys. Chem. **96**, 1530 (1992).
[27] J. S. Meth, H. Vanherzeele, and Y. Wang, Chem. Phys. Lett. **197**, 26 (1992).
[28] Z. Zhang, D. Wang, P. Ye, Y. Li, P. Wu, and D. Zhu, Opt. Lett. **17**, 973 (1992).
[29] D. Neher, G. I. Stegeman, F. A. Tinker, and N. Peyghambarian, Opt. Lett. **17**, 1491 (1992).
[30] S. C. Yang, Q. Gong, Z. Xia, Y. H. Zou, Y. Q., Wu, D. Qiang, Y. L. Sun, and Z. N. Gu, Appl. Phys. B **52**, 51 (1992).

[31] S. R. Flom, R. G. S. Pong, F. J. Bartoli, and Z. H. Kafafi, Phys. Rev. B **46**, 15598 (1992).
[32] J. Li, J. Feng and J. Sun, Chem. Phys. Lett. **203**, 560 (1993).
[33] J. Li, J. Feng and C. Sun, Int. J. Quantum. Chem. **52**, 673 (1994).
[34] N. Matsuzawa and D. A. Dixon, J. Phys. Chem. **96**, 6241 (1992).
[35] M. J. Rosker, H. O. Marcy, T. Y. Chang, J. T. Khoury, K. Hansen, and R. L. Whetten, Chem. Phys. Lett. **196**, 427 (1992).
[36] D. Jonsson, P. Norman, K. Ruud, H. Agren, and T. Helgaker, J. Chem. Phys. **109**, 572 (1998).
[37] J. R. Lindle, R. G. S. Pong, F. J. Bartoli, and Z. H. Kafafi, Phys. Rev. B **48**, 9447 (1993).
[38] N. Tang, J. P. Partanen, R. W. Hellwarth, and R. J. Knize, Phys. Rev. B **48**, 8404 (1993).
[39] W. Ji, S. H. Tang, G. Q. Xu, H. S. O. Chan, S. H. Ng, and W. W. Ng, J. Appl. Phys. **74**, 3669 (1993).
[40] F. Sun, S. Zhang, Z. Zia, Y. H. Zou, X. Chen, D. Qiang, X. Zhou, and Y. Wu, Phys. Rev. B **51**, 4614 (1995).
[41] P. Norman, Y. Lu, D. Jonsson, and H. Ågren, J. Chem. Phys. **106**, 8788 (1997).
[42] L. Geng and J. C. Wright, Chem. Phys. Lett. **249**, 105 (1996).
[43] J. Li, S. Wang, H. Yang, Q. Gong, X. An, H. Chen, and D. Qiang, Chem. Phys. Lett. **288**, 175 (1998).
[44] R. J. Knize, Opt. Commun. **106**, 95 (1994).
[45] R. H. Xie and J. Jiang, Appl. Phys. Lett. **71**, 1029 (1997).
[46] R. H. Xie and J. Jiang, Chem. Phys. Lett. **280**, 66 (1997).
[47] Y. Luo, Chem. Phys. Lett. **289**, 350 (1998).
[48] C. E. Moore, B. H. Cardelino, and X. Q. Wang, J. Phys. Chem. **100**, 4685 (1996).
[49] Z. Shuai and J. L. Bredas, Phys. Rev. B **46**, 16135 (1992).
[50] M. Fanti, G. Orlandi, and F. Zerbetto, J. Amer. Chem. Soc. **117**, 6101 (1995).
[51] M. Fanti, P. W. Fowler, G. Orlandi, and F. Zerbetto, J. Chem. Phys. **107**, 5072 (1997).
[52] R. H. Xie, J. Chem. Phys. **108**, 3626 (1998).
[53] K. Harigaya, J. Phys.: Condens. Matt., **10**, 6845 (1998).
[54] K. Harigaya, J. Lumin. **76**, 652 (1998).
[55] K. Harigaya, Synthetic Metals. **91**, 379 (1997).
[56] K. Harigaya, Japan J. Appl. Phys., **36**, L485 (1997).
[57] C. E. Moore, B. H. Cardelino, D. O. Frazier, J. Niles, and X. Q. Wang, Theochem-J. Mol. Struct. **454**, 135 (1998).
[58] H. Huang, G. Gu, S. Yang, J. Fu, P. Yu, G. K. L. Wong, and Y. Du, Chem. Phys. Lett. **272**, 427 (1997).
[59] H. Huang, G. Gu, S. Yang, J. Fu, P. Yu, G. K. L. Wong, and Y. Du, J. Phys. Chem. **102**, 61 (1998).
[60] M. J. S. Dewar, E. G. Zoebisch, E. F. Healy, and J. J. P. Stewart, J. Amer. Chem. Soc. **107**, 3902 (1985).
[61] X. G. Wan, J. M. Dong, and D. Y. Xing, J. Phys. B **30**, 1323 (1997).
[62] F. Diederich and R. L. Whetten, Acc. Chem. Res. **25**, 119 (1992).
[63] M. S. Dresselhaus, G. Dresselhaus, and R. Saito, Phys. Rev. B **45**, 6234 (1992).
[64] R. A. Jishi, M. S. Dresselhaus, and G. Dresselhaus, Phys. Rev. B **47**, 16671 (1993).
[65] R. A. Jishi, L. Venkataraman, M. S. Dresselhaus, and G. Dresselhaus, Phys. Rev. B **51**, 11176 (1995).
[66] S. Iijima and T. Ichihashi, Nature (London) **363**, 603 (1993).
[67] V. P. Dravid, X. Lin, Y. Wang, X K. Wang, A. Yee, J. B. Ketterson, and R. P. H. Chang, Science **259**, 1601 (1993).
[68] W. P. Su, J. R. Schrieffer, and A. J. Heeger, Phys. Rev. B **22**, 2099 (1990).
[69] K. Harigaya, J. Phys.: Condens. Matt. **3**, 8855 (1991).
[70] K. Harigaya and M. Fujita, Phys. Rev. B **47**, 16563 (1992).
[71] K. Harigaya and S. Abe, Phys. Rev. B **49**, 16746 (1994).
[72] J. Orr and J. F. Ward, Mol. Phys. **20**, 513 (1971).
[73] Z. Shuai and J. L. Bredas, Phys. Rev. B **46**, 4395 (1992).
[74] I. D. W. Samuel, I. Ledoux, C. Dhenaut, J. Zyss, H. H. Fox, R. R. Schrock, and R. J. Silbey, Science **265**, 1070 (1994).
[75] F. Kokai, K. Takahashi, M. Yudasaka, R. Yamada, T. Ichihashi, and S. Iijima, J. Phys. Chem. **103**, 4346 (1999), and reference therein.
[76] X. Liu, J. Si, B. Chang, G. Xu, Q. Yang, Z. Pan, S. Xie, P. Ye, J. Fan, and M. Wan, Appl. Phys. Lett. **74**, 164 (1999).
[77] K. Suenaga, M. P. Johansson, N. Hellgren, E. Broitman, L. R. Wallenberg, C. Colliex, J. E. Sundgren, and L. Hultman, Chem. Phys. Lett. **300**, 695 (1999), and references therein.
[78] T. Takahashi, S. Suzuki, T. Morikawa, H. Katayama-Yoshida, S. Hasegawa, H. Inokuchi, K. Seki, K. Kikuchi, S. Suzuki, K. Ikemoto, and Y. Achiba, Phys. Rev. Lett. **68**, 1232 (1992).
[79] N. Kurita, K. Kobayashi, H. Kumahora, and K. Tago, Phys. Rev. B **48**, 4850 (1993).
[80] N. Kurita, K. Kobayashi, H. Kumahora, K. Tago, and K. Ozawa, Chem. Phys. Lett. **198**, 95 (1992).
[81] T. Guo, C. Jin, and R. E. Smalley, J. Phys. Chem. **95**, 4948 (1991).
[82] Y. Chai, T. Guo, C. Jin, R. E. Haufler, L. P. F. Chibante, J. Fure, L. Wang, J. M. Alford, and R. E. Smalley, J. Phys. Chem. **95**, 7564 (1991).
[83] W. Andreoni, F. Gygi, and M. Parrinello, Chem. Phys. Lett. **190**, 159 (1992).
[84] Z. Chen, K. Ma, Y. Pan, X. Zhao, and A. Tang, Can. J. Chem. **77**, 291 (1999).
[85] R. H. Xie, Phys. Lett. A, **258**, 51 (1999).
[86] R. H. Xie, Z. Naturforsch. **54a**, 348 (1999).
[87] R. H. Xie, Chem. Phys. Lett. **310**, 379 (1999).
[88] J. Harris, Phys. Rev. B **31**, 1770 (1985).